JOURNAL OF AGRICULTURAL AND FOOD CHEMISTRY

Article

pubs.acs.org/JAFC

Rapid and Nondestructive Determination of Aleurone Content in Pearling Fractions of Barley by Near-Infrared (NIR) and Fluorescence Spectroscopies

Jens Petter Wold,*[,†] Diego Airado-Rodríguez,[†] Ann-Katrin Holtekjølen,[†] Ulla Holopainen-Mantila,[§] and Stefan Sahlstrøm[†]

[†]Nofima AS, Norwegian Institute for Food and Fisheries Research, Tromsø, Norway

[§]VTT Technical Research Centre of Finland, Espoo, Finland

Supporting Information

ABSTRACT: The aim of the present work was to develop and evaluate near-infrared (NIR) and fluorescence spectroscopies as rapid and potential online methods for determination of the amount of aleurone in pearling dust fractions of barley. Phytic acid was used as a marker for the aleurone layer. Different varieties of barley were pearled, and dust fractions were progressively taken out. Sample concentration of phytic acid varied in the range of 0.5−4.1 g/100 g, and highest concentrations were obtained in dust fractions for pearling degrees in the range of 15−25%. Regression models for phytic acid were developed with the same high correlations for NIR and fluorescence spectroscopies (R^2 = 0.96) and prediction errors of ±0.16−0.18 g/100 g. The models performed well on a test set of pearling fractions from two other barley varieties. The techniques are rapid and nondestructive, which means that they can be used online in connection with industrial pearling systems.

KEYWORDS: *barley, aleurone, pearling, fluorescence, NIR*

INTRODUCTION

Currently, barley processing mainly consists of dehulling, pearling, and then milling to a flour. Dehulling removes the hull and also portions of the pericarp and testa. Pearling the dehulled barley grains further removes the remaining hull, pericarp and testa, aleurone layers, and germ.[1] Dehulling and pearling are accomplished by abrasion, which subjects the grains to a rotating abrasive surface. Pearled barley typically makes up 60−70% of the total grain weight,[2] whereas the byproduct, the pearling flour (30−40%), is mainly used for animal feeds. This process is difficult to optimize to increase process yield, that is, obtain as much flour as possible with a minimum or a desired amount of fractions from the outer layers. Different properties of the barley grains, for instance, different varieties, require different pearling percentages to achieve high-quality flour and a minimum of byproduct. Practice is to adjust the pearling process according to experience or habit. Optimization of pearled barley yield and barley flour quality can, however, be solved by establishment of a rapid online method for monitoring of the pearling dust composition. Such measurements could also be used to detect and quantify particularly nutritional pearling fractions for better utilization. In this study we focused on the determination of aleurone content in the pearling dust.

Barley is known to contain certain health components. The aleurone layer is composed mainly of arabinoxylans (67−71%) and β-glucans (26%) as well as phenolic acids, vitamin E, B-vitamins, protein, triacylglycerol, minerals, phytate, and sugars.[3] Phenolic compounds, such as ferulic acid, after uptake in the gut are transported to the blood and can possibly help to reduce the destructive effect of free radicals.[4] Barley is also rich in β-glucan, a polysaccharide building block of the cell walls in the aleurone layer and the endosperm, which is approved by EFSA to reduce the cholesterol level and sugar in the blood after a meal.[5] Holtekjølen et al.[6] found that the pearling flour is a potential natural source of phytochemicals with antioxidant effects. Chemical characterization of different pearling fractions of barley was done by Blandino et al.,[7] who found that the total antioxidant activity (TAA) in the 15−25% pearling fraction was significantly higher than in the other fractions. The inclusion of this fraction in the preparation of bread increased TAA and dietary fibers without impairing the physical bread properties. For milling companies it can be important to be able to quantitate the amount of kernel tissues and health-promoting components in their milling fractions, for example, the content of hull, soluble fiber (β-glucan), and aleurone layer, and in that way create a competitive advantage in terms of diversifying milling and bakery product ranges. Ultimately, consumers will benefit from a naturally produced healthier product.

Barron et al.[8] isolated barley grain tissues from both hulled and hulless barley for chemical analyses. They found that phytic acid is specifically localized in the aleurone layer and that it can be used as a marker for this tissue among other grain tissues. They also identified the phenolic compound *p*-coumaric acid as an efficient marker of the hull and proposed that it could be used to monitor the dehulling process.

To perform continuous product or process control, rapid analytical techniques are required. Traditional chemical methods typically require several hours or days, and such a

Received: November 4, 2016
Revised: February 1, 2017
Accepted: February 7, 2017
Published: February 7, 2017

DOI: 10.1021/acs.jafc.6b04954
J. Agric. Food Chem. XXXX, XXX, XXX−XXX

time span is rarely applicable in modern production. Spectroscopic instrumentation has gained popularity in processing industries during the past two to three decades, being rapid, reliable, and nondestructive analytical techniques. For online use in food production, near-infrared (NIR) spectroscopy is probably the most widely used spectroscopic technique. The near-infrared part of the electromagnetic spectrum comprises overtones and combination bands of fundamental bond vibrations found in the infrared region. The molecular bonds that absorb in the NIR region are mainly −O−H, −C−H, −N−H, and −S−H, reflecting molecular structural characteristics of proteins, carbohydrates, lipids, and water. NIR is established in the milling industry for at-line and online determination of typically moisture, protein, fat, and ash in flour and whole grains. Promising results for the determination of β-glucan have been obtained.[9] It is also reported that phytic acid has a distinct absorption spectrum in the NIR region and that it can be determined in green gram seeds and cotton seeds by NIR spectroscopy.[10,11] NIR is therefore a promising method for continuous monitoring of the pearling fractions, where the amount of, for example, protein, β-glucan, and phytic acid will vary systematically through the different kernel layers.[7]

It is well-known that different tissues of the grains have characteristic fluorescent properties. The strong bluish fluorescence from the aleurone layer comes mainly from ferulic acid.[12] Jensen et al.[13] showed that endosperm emits fluorescence in the UV typical for tryptophan and that pericarp has a distinct green-yellow fluorescence peaking at about 520 nm with unknown origin. They also demonstrated that it is possible to quantitate the amount of pericarp, aleurone, and endosperm in wheat milling fractions by the use of autofluorescence spectra and multivariate calibration. The spectroscopic measurements were performed on 20 mg of flour samples suspended in glycerol and water. Symons and Dexter[14] used fluorescence imaging in pilot mill streams to monitor aleurone and pericarp as an estimator of flour refinement. Pericarp fluorescence correlated especially well with flour refinement and indicated promise for online quality evaluation in mills.

The main aim of the present work was to develop and evaluate a rapid and preferably online method for the determination of the amount of aleurone layer in pearling fractions of barley. Such a method could be used to control the pearling process toward maximum yield as well as extract fractions with high aleurone content for use in certain products. We have tested and compared two rapid spectroscopic techniques, which both have potential for online use: NIR and fluorescence spectroscopies. Different varieties of barley were pearled, and dust fractions were systematically taken out over time. As reference marker for the aleurone layer we used phytic acid. Concentrations of different phenolic acids were also determined. Multivariate regression as well as spectroscopic curve resolution were used to analyze the data and make calibration models.

MATERIALS AND METHODS

Materials. For the investigations, three separate sample sets of pearling dust were produced. The sample sets were made as follows.

Sample Set 1. A J. E. Barley Huller (Glenn A. Burdick, Minneapolis, MN, USA) pearler was used to make 12 fractions each of two different barley varieties, 'Marigold' and 'Olve'. The pearler consists of a wire brush that presses small particles through a sieve. A maximum of 20 g of grain could be pearled at a time. The dust fractions were made by collecting pearling dust systematically according to time of pearling. The fractions were collected for 0−30, 30−60, 60−90, ..., 330−360 s. A total of 24 samples were produced.

Sample Set 2. A Testing Mill TM05 (Satake, Stafford, TX, USA) with abrasive stone 30 was used to make 9 fractions each from two parallels of 200 g of 'Marigold' kernels and then 10 fractions each of two 200 g parallels of 'Olve' kernels. A total of 38 samples were produced. Progressive pearling fractions were taken after approximate pearling degrees of 9, 14, 18, 22, 26, 30, 33, 38, 42, and 49%.

Sample Set 3. The same Satake Testing Mill TM05 was used to make eight fractions each from two parallels of 200 g of 'Pihl' kernels and then eight fractions each of two 200 g parallels of 'Pirona' kernels. 'Pihl' and 'Pirona' are hulless barley varieties. A total of 32 samples were produced. Progressive pearling fractions were taken after approximate pearling degrees of 5, 10, 15, 21, 26, 31, 36, and 40%.

Spectroscopic Measurements. NIR spectra in reflection mode were obtained directly on intact dust samples with a DA7200 spectrometer (Perten Instruments, Hägersten, Sweden). Samples were disposed in a circular sampling cup, and measured area was approximately 30 cm^2. Sampling time was set to 6 s, and spectra were registered by covering every fifth wavelength in the region of 950−1650 nm. Each sample was measured in triplicate, and the average spectrum was used for further analysis.

Fluorescence spectra were also collected from the intact pearling dust samples. Samples were placed in black circular sample cups, which exposed a flat circular surface with a diameter of 5 cm for the measurements. Measurements were carried out with a Fluoromax-4 spectrofluorometer (Horiba Scientific, Kyoto, Japan) in front face mode via a FL-300/FM4-3000 bifurcated fiber-optic probe (Horiba Scientific). The distance between the probe head and the sample was about 5 cm and created a circular measurement area of 40 mm diameter. Probe and sample were covered by a black shield to avoid ambient straylight. Three different excitation wavelengths were employed to register emission spectra of each sample. Samples were sequentially illuminated with 470, 350, and 280 nm excitation light, and the corresponding fluorescence emission spectra were registered in the ranges of 490−650, 400−600, and 300−540 nm, respectively. The three assayed excitation wavelengths were systematically applied in decreasing order to minimize potential sample alteration by the UV excitation. The selected excitation wavelengths should enable detection of pericarp, aleurone, and endosperm, respectively.[13,14]

Determination of Phytic Acid. Phytic acid was used as a marker for the aleurone layer and was measured for all samples. It was determined by means of a K-PHYT phytic acid (phytate)/total phosphorus assay kit (Megazyme, Chicago, IL, USA). This method involves acid extraction of inositol phosphates followed by treatment with a phytase that is specific for phytic acid (IP6) and the lower *myo*-inositol phosphate forms (i.e., IP2, IP3, IP4, IP5). Subsequent treatment with alkaline phosphatase ensures the release of the final phosphate from *myo*-inositol phosphate (IP1), which is relatively resistant to the action of phytase. The total phosphate released is measured using a modified colorimetric method and given as grams of phosphorus per 100 g of sample material.

Determination of Phenolic Acids. Total phenolic acids (ferulic acid, caffeic acid, *p*-coumaric acid, and sinapic acid) were determined for four series of pearling fractions, one each from 'Olve', 'Marigold', 'Pihl', and 'Pirona'. Extraction of total phenolic acids was performed as described earlier.[15] Identification and quantitation of phenolic acids were carried out using a UltiMate 3000 rapid separation high-performance liquid chromatography (HPLC) system with a 3000 RS diode array detector (Dionex, Sunnyvale, CA, USA) and an Acquity UPLC BEH C8, 1.7 μm, 2.1 × 150 mm column (Waters, Milford, MA, USA). A gradient elution program was used with 1% acetic acid in Milli-Q water as eluent A and 1% acetic acid in acetonitrile as eluent B. The injection volume was 10 μL, and the flow rate was 0.450 mL/min, with a column temperature of 50 °C. The gradient elution program was as follows: 5% B (0 min), 5% B (0.8 min), 10% B (1.2 min), 10% B (1.9 min), 15% B (2.4 min), 15% B (3.7 min), 21% B (4.0 min), 21% B (5.2 min), 27% B (5.7 min), 50% B (8.0 min), 100% B (9.0

DOI: 10.1021/acs.jafc.6b04954
J. Agric. Food Chem. XXXX, XXX, XXX−XXX

min), 100% B (12.5 min), 5% B (15.0 min), 5% B (20.0 min). Initial conditions were used for 10 min of equilibration before a new analysis was started. The identification and quantitation of phenolic acids were carried out using external standards (caffeic, *p*-coumaric, ferulic, and sinapic acid) and UV spectrum characteristics with the Chromeleon chromatography information management System (Dionex).[16]

Microscopy of Pearled Barley Grains. Selected grains of cultivars 'Marigold', 'Olve', 'Pihl', and 'Pirona' representing various pearling times were subjected to microscopy to evaluate the effect of pearling on the aleurone layer. A quick staining method was developed for this examination of aleurone layer in pearled grains. Grains were cut in half cross-sectionally in the middle of the grain. Cross-cut surfaces of individual grains were stained with 0.1% (w/v) acid fuchsin (BDH Chemicals Ltd., Poole, UK) in 1% acetic acid for 1 min and rinsed twice with water. Stained grains were then dried in the dark for 30 min. The cross-cut surfaces were imaged using excitation wavelength (330−380 nm) and emission from 420 nm with an AxioImager M.2 microscope (Carl Zeiss GmbH, Göttingen, Germany). Under these lighting conditions, aleurone cell walls were detected as bright blue due to autofluorescence of phenolic substances present in cell walls, whereas starchy endosperm appeared bright red. Micrographs were obtained using a Zeiss Axiocam 506 CCD color camera (Zeiss) and Zen imaging software (Zeiss). In addition to epifluorescence microscopy, the grains were imaged using a SteREO Discovery.V8 stereomicroscope equipped with Achromat S 0.5× objective (Carl Zeiss MicroImaging GmbH) and an Olympus DP-25 single-chip color CCD camera (Olympus Life Science Europa GmbH, Hamburg, Germany). Approximately 18−20 grains/sample were examined, and representative images were chosen for publication.

Data Analysis. *Pretreatment of Spectroscopic Data.* NIR spectra are affected by differences in sample scattering. Differences in scattering can occur due to the use of different pearling systems. To reduce the effect of such phenomena, the NIR spectra were normalized by standard normal variate (SNV)[17] prior to calibration.

The fluorescence spectra were normalized by unit area normalization, meaning that the area under each spectrum equals 1. This was done separately for emission spectra for the different excitations. This normalization removes the main intensity variations and emphasizes the shapes of the spectra.

Calibration. Partial least-squares regression (PLSR)[18] was used to make calibrations between spectroscopic data and the reference values of phytic acid. Separate and common models for samples in sample sets 1 and 2 were made. Sample set 3 was used as a test set.

The optimal number of PLSR factors of the calibration models was determined by full cross-validation. The predicted value for each sample, $\hat{y}_i$, was compared with the reference value, y_i (nominal phytic acid concentration). The squared multivariate correlation coefficient (R^2), which describes the relationship between the measured and the predicted values of the y variable, and the prediction error of the regression model, expressed as root-mean-square error of either cross-validation (RMSECV), were used to evaluate the model performance. RMSECV is defined as

$$\mathrm{RMSECV} = \sqrt{\frac{1}{N}\sum_{i=1}^{N}(y_i - \hat{y}_i)^2}$$

where i denotes the samples from i to N.

The obtained calibration models were used to predict phytic acid concentration in the test set samples. Model performance was reported as the root-mean-square error of prediction (RMSEP), calculated exactly as RMSECV ($\hat{y}_i$ being result of prediction and not cross-validation), and the multivariate correlation coefficient (R^2). PLSR and spectroscopic preprocessings were performed with the software The Unscrambler, ver. 9.8 (Camo AS, Oslo, Norway).

Multivariate Curve Resolution (MCR). Fluorescence spectra lend themselves to curve resolution. MCR enables extraction of potential pure spectroscopic components originating from the different inherent fluorophores and their respective concentrations. The obtained concentrations for MCR components were compared with reference analyses. A non-negativity constraint was applied in the spectra and concentration modes to obtain a realistic solution. The algorithm for MCR has previously been described in detail.[19,20] MCR was carried out with the software The Unscrambler, ver. 9.8 (Camo AS).

RESULTS AND DISCUSSION

Detection of the Effect of Pearling on Grain Layers by Microscopy. The effect of pearling on barley grain outer layers was verified by microscopy. For this, grains of four barley varieties studied with various degrees of pearling were examined. In Figure 1, the appearance of native and pearled barley kernels of 'Olve' and the cross-cut surfaces of corresponding kernels stained with Acid Fuchsin are presented. Stereomicroscopy images showed that pearling first removed the hull and proceeded then gradually toward the center parts of the grain. However, the ends of the kernels seemed to be more readily pearled than the sides.

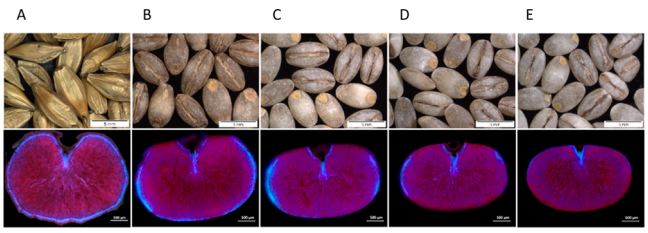

Figure 1. Stereomicrographs (upper panel) and epifluorescence micrographs (lower panel) of grains (cv. 'Olve') with different degrees of pearling: (A) native, unpearled grain; grains with pearling degree of 14% (B), 27% (C), 32% (D), and 39% (E). In epifluorescence images, the aleurone layer appears bright blue surrounding starchy endosperm stained red. Scale bars represent 5 mm and 500 μm in the lower and upper panel images, respectively.

The images of the stained cross-cut surfaces revealed that aleurone appearing blue due to autofluorescence was first removed from the ventral side of the grain, excluding the ventral furrow (Figure 1B), and then from the dorsal side (Figure 1C). This was followed by the removal of the aleurone in the flanks of the kernels. The aleurone layer located in the ventral furrow was not removed even with a pearling degree of 39% (Figure 1E). In general, it was noted that pearling of hulled and hulless barley kernels followed a similar pattern, although the aleurone layer of hulless varieties was removed at a slightly lower degree of pearling than that of hulled varieties (data not shown).

Phytic Acid in Pearling Fractions. Figure 2 shows the concentration of phytic acid in the obtained dust fractions in the three sample sets. It was expected that the concentration of phytic acid should increase in the dust fractions from the beginning of the pearling and then decrease after passing the aleurone layer. In the first trial (sample set 1) the concentration of phytic acid versus degree of pearling showed a quite flat appearance, which indicated that the aleurone layer was not concentrated in a few dust fractions. It became obvious that the pearling did not remove all of the aleurone, because a clear decrease with pearling time was not observed. It turned out that the pearling system used was not very efficient. For the second trial (sample set 2), a different pearling system was used, and in this case, it was observed that the concentration of phytic acid did indeed decrease with longer pearling times. This difference indicated that the second pearling system was more efficient than the first one. The aleurone was distributed more or less

DOI: 10.1021/acs.jafc.6b04954
J. Agric. Food Chem. XXXX, XXX, XXX−XXX

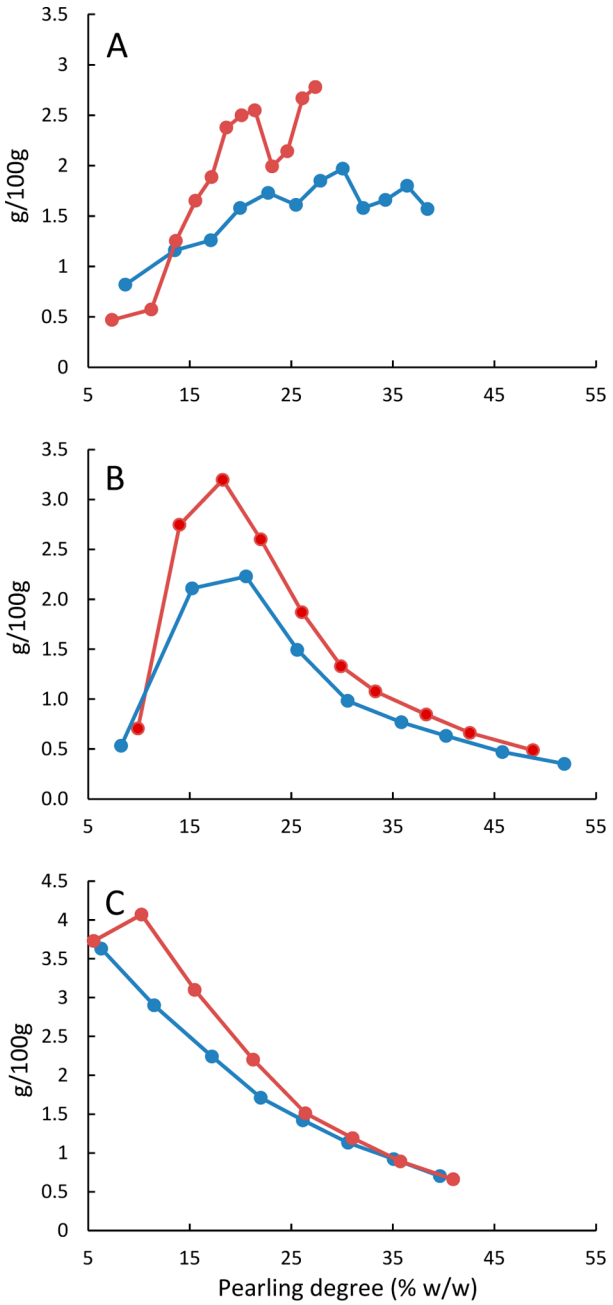

Figure 2. Concentration of phytic acid in pearling fractions from (A) 'Olve' (red) and 'Marigold' (blue) (sample set 1), (B) 'Olve' (red) and 'Marigold' (blue) (sample set 2), and (C) 'Pihl' (blue) and 'Pirona' (red) (sample set 3).

across all fractions, but highest concentrations were obtained for pearling yields in the 13−25% range. This result corresponds with Blandino et al.,[7] who found that the 15−25% pearling fractions of barley had the highest antioxidant activity, which most likely was due to the antioxidants in the aleurone layer. It should also be mentioned that the measured concentrations of phytic acid were higher for the variety 'Olve' than for 'Marigold'. In the third trial (sample set 3) on hulless barley, there was an immediate high concentration of phytic acid due to very thin layers of pericarp and testa. A gradual decrease comparable with that of sample set 2 then occurred. The levels of phytic acid in the two varieties 'Pihl' and 'Pirona' were quite similar.

Phenolic Acids in Pearling Fractions. Concentrations of ferulic acid, caffeic acid, *p*-coumaric acid, and sinapic acid in one pearling series of 'Olve' and 'Marigold' from sample set 2 are shown in Figure 3. The evolution of the concentrations of caffeic and sinapic acid with pearling degree followed a pattern similar to the concentration of phytic acid, although the maximum concentrations were reached at slightly lower pearling degrees than phytic acid. Ferulic and *p*-coumaric acid followed different patterns, which are related to their distribution along the different layers of the grain. The concentration of ferulic acid continuously decreased at an approximately constant rate for pearling degrees between 10 and 50%. This corresponds with Ndolo et al.,[21] who found that the concentrations of ferulic acid in the pericarp and aleurone in the two barley varieties were high, but much lower in the endosperm. Thus, the more endosperm entering the pearling fraction, the more the concentration of ferulic acid will decrease. Even though ferulic acid is responsible for the strong bluish fluorescence in the aleurone layer, the concentrations are also high in the pericarp tissue, which does not exhibit this strong blue fluorescence. With regard to *p*-coumaric acid, its maximum concentration in dust is obtained at the beginning of the pearling process, indicating that highest concentrations are found in the pericarp. These profiles suggest that the concentrations of *p*-coumaric and ferulic acid are not the best markers for the aleurone layer. This is in agreement with results obtained after isolation of barley grain tissues from both hulled and hulless barley for chemical analyses of biomarkers.[8]

Spectroscopic Measurements. Figure 4 shows typical NIR spectra from dust fractions ('Olve' from sample set 2). For unprocessed absorption spectra, the highest offset was obtained for the first fraction, and then the offset steadily decreased with increasing pearling time. This systematic variation in offset is probably due to a corresponding variation in light scattering in the samples. The color of the samples also varied systematically from dark to white with pearling time; however, color should not affect NIR spectra much in this spectral region. For scatter-corrected spectra the systematic offset disappeared, but clear systematic changes with pearling time could be observed around 1100 and 1200 nm.

Figure 5 shows typical emission fluorescence spectra from dust fractions at the three assayed excitation wavelengths. The emission spectra for excitation at 280 nm showed a main maximum centered at 320 nm and a small shoulder around 438 nm. The emission spectra for excitation at 360 nm was less intense and had a single maximum centered at 435 nm, slightly broader than the main maximum of the former one. Finally, the emission spectra for λ_{ex} 470 nm in some cases presents a maximum at 544 nm and in other cases presents a quite flat aspect with no maxima. For each sample set, the series of spectra registered at λ_{ex} 280 nm, showed a systematic increase from the first to the last fraction. For λ_{ex} 360 nm, there was an increase at the start and then a decrease, whereas for λ_{ex} 470 nm there appeared to be a quite steady decrease with pearling time. For regression analysis as well as MCR we used all three emission spectra concatenated as shown in Figure 5.

Calibration Results. Table 1 summarizes calibration results for NIR spectroscopy for sample sets 1 and 2. It is clear that quite good regression models could be established for phytic acid in the pearling fractions. The two sample sets behaved differently, and better models were obtained for sample set 2. The two sample sets were produced by different pearling machines, and this might be why different results were obtained

DOI: 10.1021/acs.jafc.6b04954
J. Agric. Food Chem. XXXX, XXX, XXX−XXX

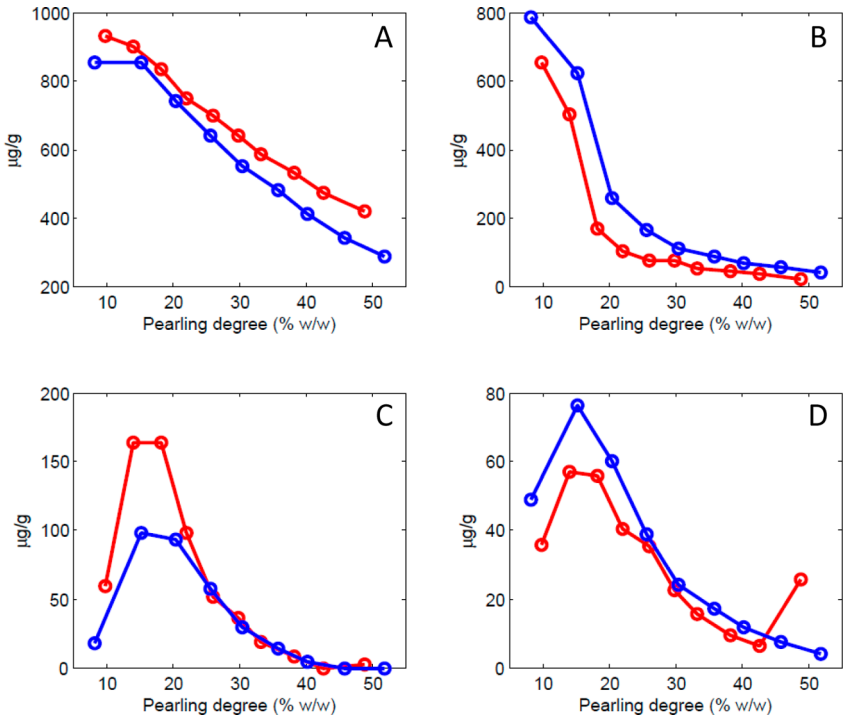

Figure 3. Concentrations of (A) ferulic acid, (B) *p*-coumaric acid, (C) caffeic acid, and (D) sinapic acid in pearling fractions from 'Olve' (red) and 'Marigold' (blue) from sample set 2.

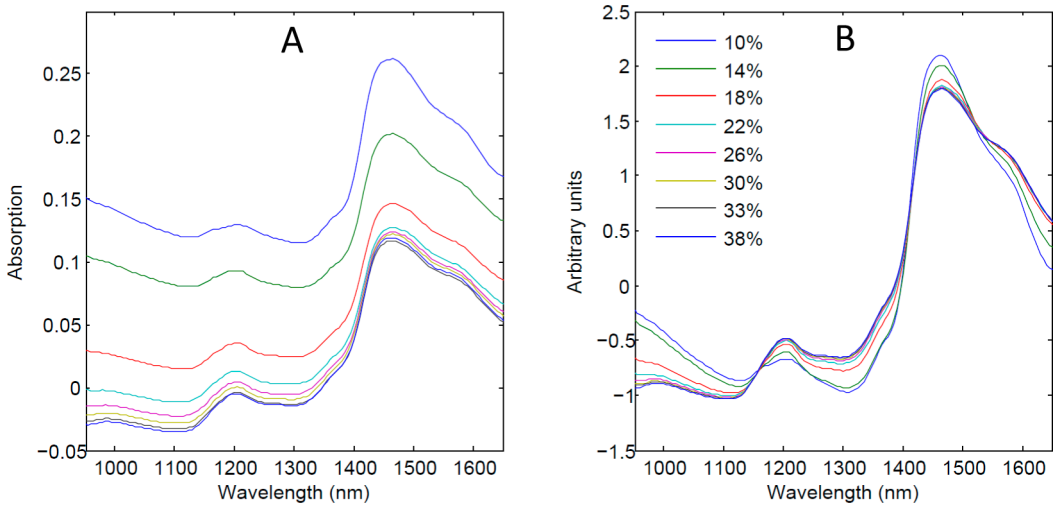

Figure 4. NIR spectra from dust fractions after pearling: absorption spectra (left); SNV-corrected spectra (right). Line colors indicate different pearling degrees.

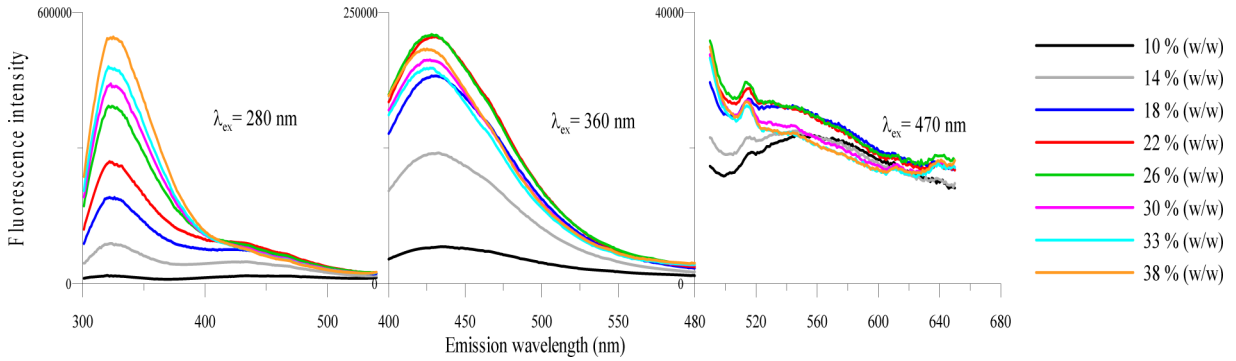

Figure 5. Fluorescence spectra from dust fractions after pearling. Line colors indicate different pearling degrees.

DOI: 10.1021/acs.jafc.6b04954
J. Agric. Food Chem. XXXX, XXX, XXX−XXX

Table 1. Results for Regression Models Based on NIR Cross-Validated Models

pearling data set	spectral data	no. of PLSR comp	R^2	RMSECV
sample set 1	NIR absorption	2	0.86	0.23
	NIR SNV	4	0.85	0.24
sample set 2	NIR absorption	5	0.94	0.20
	NIR SNV	6	0.96	0.16
sample set 1 + sample set 2	NIR absorption	7	0.87	0.28
	NIR SNV	8	0.89	0.26
sample set 1	fluorescence	2	0.85	0.23
	fluorescence norm	3	0.85	0.24
sample set 2	fluorescence	5	0.95	0.18
	fluorescence norm	4	0.96	0.18
trials 1 + 3	fluorescence	5	0.92	0.22
	fluorescence norm	5	0.87	0.28

and also why the two sample sets were not well modeled together. Attempts to remove the main spectral variation due to differences in light scattering properties did not significantly improve the model where the two data sets were combined. The best model was obtained for sample set 2 after SNV correction of the spectra. This model required one PLS factor more than the model based on raw absorption spectra, and this suggests that SNV enables modeling of more subtle spectral changes. An R^2 of 0.96 and a prediction error (RMSECV) of 0.16% are acceptable for the kind of process application we are aiming at. On the basis of the regression coefficients (not shown) it is not easy to identify the main chemical sources of information for the model; however, several are probably contributing. Phytic acid has a distinct signature in the NIR region.[10] The amount of bran, protein, and β-glucan will vary systematically in these fractions, and NIR is sensitive to all of them.[9,22]

The results for fluorescence spectroscopy are quite similar to those of NIR (Table 1). Better results for sample set 2 than for sample set 1 were also obtained now, and the combination of the two data sets led to slightly more complex models. The unit area normalization did not give notably better calibration models, and for the combined data set the performance was worse than for raw fluorescence spectra. This suggests that the actual fluorescence intensity is important for the modeling. Common for NIR and fluorescence was that models for data set 2 required more components than did data set 1. This indicates that sample set 2 contained some spectral variation that was not present in sample set 1. Because poorer models for phytic acid were obtained for sample set 1 for both NIR and fluorescence, there might have been some mismatch between the spectroscopic data and the reference values. From Figure 2 is can be seen that phytic acid in sample set 1 varied up and down in an unexpected way as a function of pearling degree.

It is reasonable that fluorescence can be used to indirectly measure the amount of phytic acid because it is a marker for the aleurone layer. As pointed out above, pericarp, aleurone, and endosperm have distinct and different fluorescent properties.[13] Different phenolic acids in the aleurone are fluorescent, for instance, ferulic acid, caffeic acid, sinapic acid, and *p*-coumaric acid (Figure 3).[23] Phytic acid is, however, to our knowledge not fluorescent.

The chemical foundation for the calibrations (both NIR and fluorescence) is not completely clear. It was therefore important to validate these models on independent samples. Table 2 summarizes how the prediction models based on

Table 2. Results for Prediction of Test Set

pearling data set	spectral data	R^2	RMSEP	offset
NIR	absorption	0.95	1.47	−1.04
	SNV	0.97	0.35	0.17
fluorescence	raw fluorescence	0.49	1.14	2.20
	unit area norm	0.97	0.36	0.65

sample set 2 performed on sample set 3, which were made of two other barley varieties. The models for sample set 2 were used because sample sets 2 and 3 were produced by the same pearling system. It can be seen that except for the model based on raw fluorescence data, the correlations between the predicted and measured values of phytic acid were high (0.95−0.97). For all of the models there were unwanted issues with offsets or biases compared to the reference values, but Figure 6 shows that the predicted values were quite accurate and useful. All of the predicted values were in the right concentration range and followed the same trend with pearling degree as did measured phytic acid. On samples from 'Pihl', the NIR predicted values were very close to the reference values, whereas for those from 'Pirona' the predicted values were systematically below. The fluorescence model performed at about the same level as NIR.

There are differences between varieties of barley, and for the optical measurements described here, this can probably result in systematic offsets as seen for the NIR predictions for 'Pirona'. That means that for process purposes, it might be necessary to follow the progression of the pearling dust during pearling rather than to rely on absolute values.

The model based on raw fluorescence spectra did not perform well on the test samples, whereas the normalized spectra worked well. This indicates that the shape of the spectra is more important than the actual intensity. Preprocessing of fluorescence spectra from front face measurements of intact biosamples for quantitative modeling is not a well-explored topic and should be more thoroughly elucidated.

Multivariate Curve Resolution. MCR was attempted only on fluorescence data, because these spectra apparently consisted of rather few spectral components. Normalized fluorescence spectra from sample sets 2 and 3 were together subjected to MCR, and three dominant spectral components were found (Figure 7). On the basis of these components their relative concentrations could be estimated, shown in Figure 8 for a set of pearling fractions for each of the varieties 'Olve', 'Marigold', 'Pihl', and 'Pirona'. One component shows a maximum at 335 nm for excitation at 280 nm, which probably originates from tryptophan with possible contributions from tyrosine and phenylalanine. The estimated concentrations for this component increase steadily with pearling time and indicate the amount of endosperm in the fractions. The second component has a maximum emission around 430 nm for excitation at 280 nm and at about 445 nm for excitation at 350 nm. These are typical properties for phenolic acids. The concentration of this component tends to follow a quite similar course to phytic acid and the aleurone layer (Figure 2). The third spectral component has a broad maximum around 550 nm for excitation at 470 nm, and it decreased quite rapidly with

DOI: 10.1021/acs.jafc.6b04954
J. Agric. Food Chem. XXXX, XXX, XXX−XXX

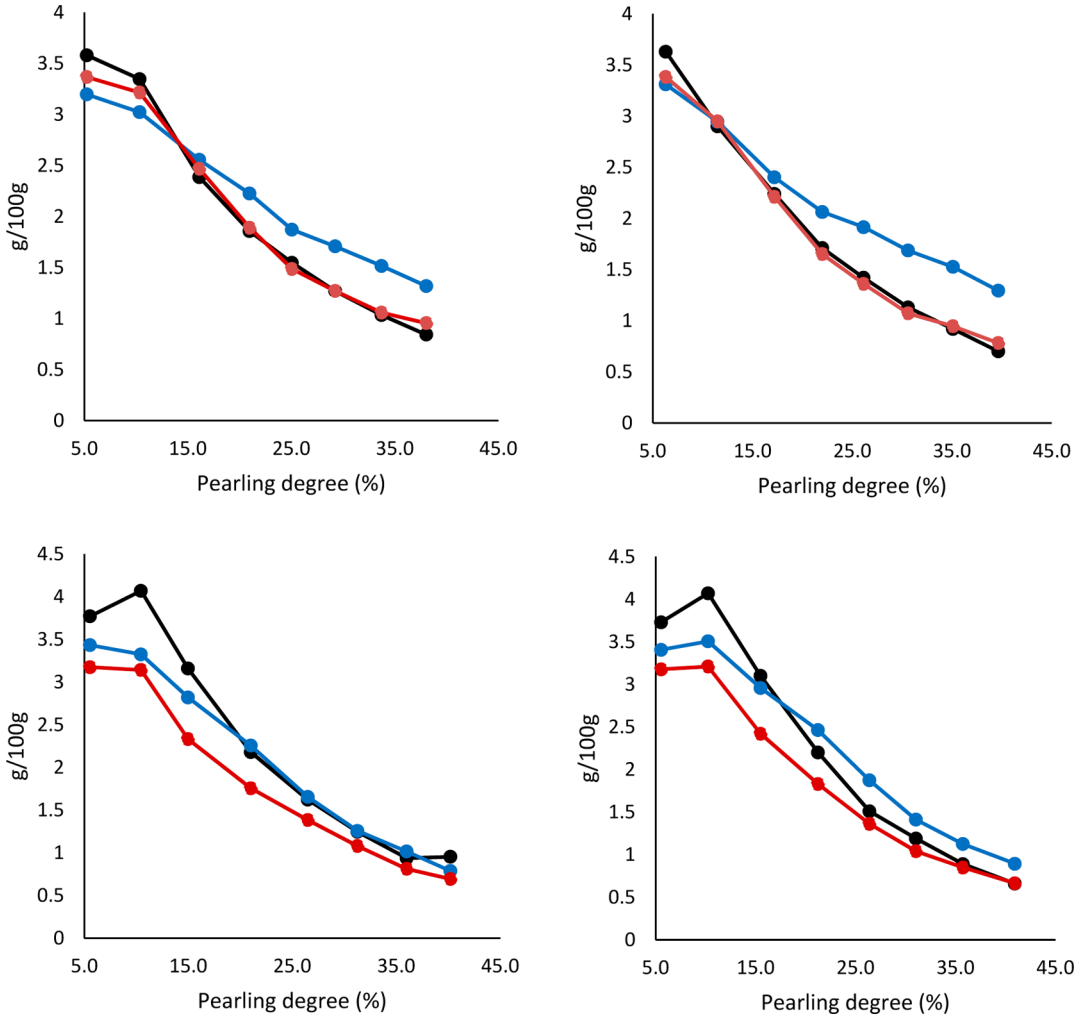

Figure 6. Predicted phytic acid in 32 pearling fractions of barley varieties 'Pihl' (upper panel) and 'Pirona' (lower panel): referenced phytic acid (black line); predicted by fluorescence (blue line); predicted by NIR (red line).

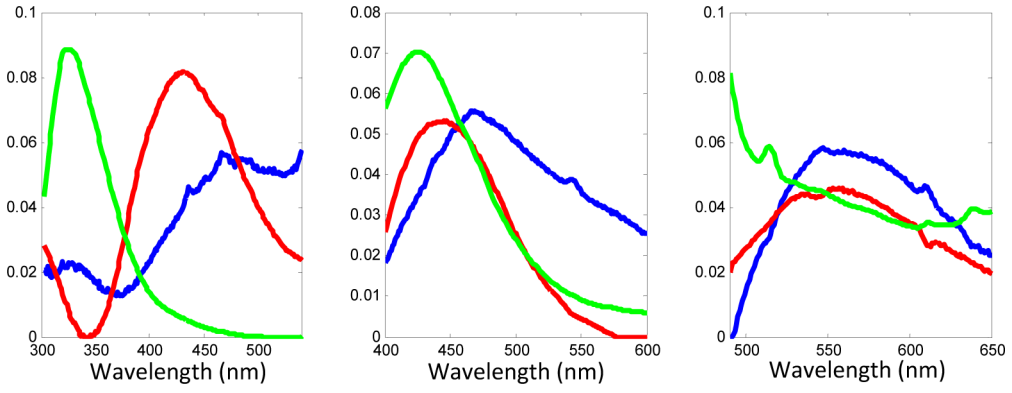

Figure 7. Estimated spectral components from fluorescence spectra by MCR: component 1 (green); component 2 (red); component 3 (blue).

pearling time. The identification of this component is not clear; however, it has previously been detected in pericarp.[13]

The estimated concentrations for the second component correlated well with the concentrations of phytic acid, ferulic acid, and caffeic acid (0.95, 0.95, and 0.98, respectively) for the 'Pihl' and 'Pirona' samples. For sample set 2, 'Olve' and 'Marigold', the corresponding correlations were lower (0.64, 0.88, and 0.73, respectively) mainly due to mismatch with the first pearling fraction in every pearling series. If these were removed from the data set, the correlations increased notably (0.90, 0.90, and 0.93, respectively). It is clear that the intensity of fluorescence from the outer pericarp does not correlate well with the amount of phenolic acids. Even though the fluorescent ferulic acid is present in the pericarp, the fluorescence is very low. A reason might be that the fluorescence is quenched or reabsorbed by other molecules in this tissue.

Overall, the results illustrate that it is possible to decompose rather complex fluorescence spectra from intact pearling

DOI: 10.1021/acs.jafc.6b04954
J. Agric. Food Chem. XXXX, XXX, XXX−XXX

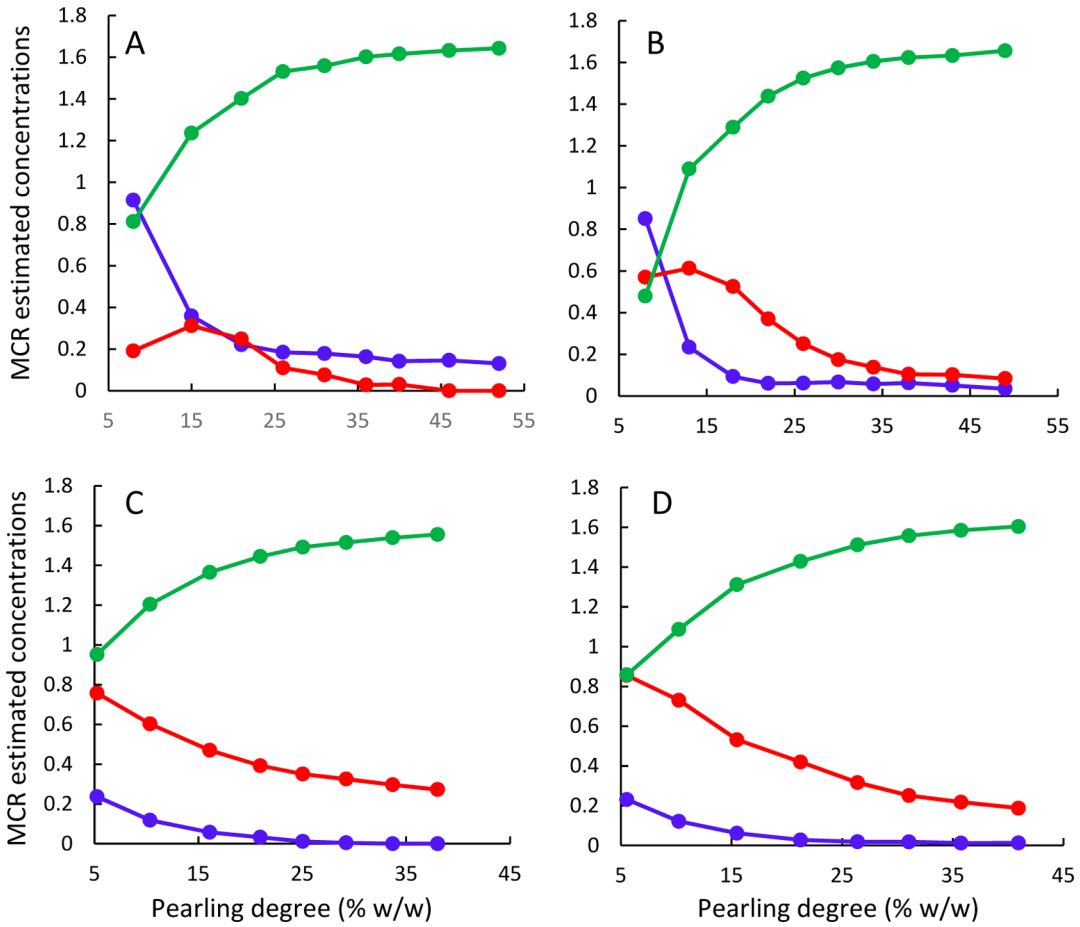

Figure 8. Estimated concentrations of MCR components based on fluorescence spectra from different barley varieties: (A) 'Marigold'; (B) 'Olve'; (C) 'Pihl'; (D) 'Pirona'; component 1 (green); component 2 (red); component 3 (blue).

fractions into approximate concentrations of aleurone, endosperm, and pericarp. This approach is excellent for interpretation of the spectroscopic data and might also be used for continuous and semiquantitative process monitoring.

The results from this work indicate that it is possible to estimate the amount of phytic acid and, therefore, the amount of aleurone in pearling dust fractions from barley by both NIR and fluorescence spectroscopies. The techniques are rapid, and no sample pretreatment is required, which means that they can be used online in connection with industrial pearling systems. NIR is well established in the cereal industry, and suitable equipment is available for online use on flour streams. A system for fluorescence spectroscopy would in principle be easy to make, but might not presently be ready available off the shelf. In this work we used concatenated emission spectra for three different excitations, but it might be sufficient to use two or even just one excitation. On the basis of modeling, the 280 nm excitation was the most informative, then 350 nm, and 470 nm the least informative.

There are systematic differences between barley varieties. For example, 'Olve' seems to contain more phytic acid than 'Marigold' (Figure 2B), and 'Pirona' might contain more than 'Pihl'. This means that an aleurone peak in dust fractions of 'Olve' will have a higher phytic acid content than the corresponding fractions from 'Marigold'. The level of phytic acid in the grains at hand must probably be monitored over time in the process before process optimization can be performed.

An online system can be used to adjust the pearling time for each batch to optimize the amount and flour quality and to minimize the amount of pearling dust. One can also envision specially designed pearling systems where it can be possible to follow the pearling process and automatically extract fractions with high concentrations of aleurone and at the same time control the process toward optimal utilization of the raw material.

■ ASSOCIATED CONTENT

Supporting Information

The Supporting Information is available free of charge on the ACS Publications website at DOI: 10.1021/acs.jafc.6b04954.

Predicted versus measured phytic acid content in dust samples from sample set 2 based on NIR spectra (PDF)

■ AUTHOR INFORMATION

Corresponding Author

*(J.P.W.) Phone: +47 95979749. Fax: +47 64940333. E-mail: jens.petter.wold@nofima.no.

ORCID

Jens Petter Wold: 0000-0003-1819-5195

Ulla Holopainen-Mantila: 0000-0003-1109-0569

Funding

This work was partially funded by the EU project BarleyBoost and the Norwegian Agricultural Food Research Foundation through the projects Food Imaging (Project 225347/F40) and

DOI: 10.1021/acs.jafc.6b04954
J. Agric. Food Chem. XXXX, XXX, XXX−XXX

Food for Health−Dietary fibre and glycaemic carbohydrates (Project 225352/F40).

Notes

The authors declare no competing financial interest.

■ ACKNOWLEDGMENTS

We thank Hanne Zobel for skilled technical assistance.

■ REFERENCES

(1) Izydorczyk, M. S.; Symmons, S. J.; Dexter, J. E. Fractionation of wheat and barley. In *Whole-Grain Foods in Health and Desease*; Marquart, L. M., Slavin, J. L., Fulcher, R. G., Eds.; American Association of Cereal Chemists: St. Paul, MN, USA, 2002.

(2) Jadhav, S. J.; Lutz, S. E.; Ghorpade, V. M.; Salunkhe, D. K. Barley: chemistry and value-added processing. *Crit. Rev. Food Sci. Nutr.* **1998**, *38*, 123−171.

(3) Hemery, Y.; Rouau, X.; Lullien-Pellerin, V.; Barron, C.; Abecassis, J. Dry processes to develop wheat fractions and products with enhanced nutritional quality. *J. Cereal Sci.* **2007**, *46*, 327−347.

(4) Hemery, Y.; Lullien-Pellerin, V.; Rouau, X.; Abecassis, J.; Samson, M. F.; Åman, P.; von Reding, W.; Spoerndli, C.; Barron, C. Biochemical markers: Efficient tools for the assessment of wheat grain tissue proportions in milling fractions. *J. Cereal Sci.* **2009**, *49*, 55−64.

(5) EFSA.. Scientific Opinion on the substantiation of health claims related to beta-glucans from oats and barley and maintenance of normal blood LDL-cholesterol concentrations (ID 1236, 1299), increase in satiety leading to a reduction in energy intake (ID 851, 852), reduction of post-prandial glycaemic responses (ID 821, 824), and "digestive function" (ID 850) pursuant to Article 13(1) of Regulation (EC) No. 1924/20061. *EFSA J.* **2011**, *9*, 2207.

(6) Holtekjølen, A. K.; Sahlstrøm, S.; Knutsen, S. H. Phenolic contents and antioxidant activities in covered whole-grain flours of Norwegian barley varieties and in fractions obtained after pearling. *Acta Agric. Scand., Sect. B* **2011**, *61*, 67−74.

(7) Blandino, M.; Locatelli, M.; Sovrani, V.; Coïsson, J. D.; Rolle, L.; Travaglia, F.; Giacosa, S.; Bordiga, M.; Scarpino, V.; Reyneri, A.; Arlorio, M. Progressive pearling of barley kernel: chemical characterization of pearling fractions and effect of their inclusion on the nutritional and technological properties of wheat bread. *J. Agric. Food Chem.* **2015**, *63*, 5875−5884.

(8) Barron, C.; Holopainen-Mantila, U.; Sahlstrøm, S.; Holtekjølen, A. K.; Lullien-Pellerin, V. Assessment of biochemical markers identified in wheat for monitoring barley grain tissue. *J. Cereal Sci.* **2017**, in press.741110.1016/j.jcs.2017.01.004 Barron, C.; Holopainen-Mantila, U.; Sahlstrøm, S.; Hotekjølen, A. K.; Lullien-Pellerin, V. Assessment of biochemical markers identified in wheat for monitoring barley grain tissue. *J. Cereal Sci.* **2017**, *74*, 11.

(9) Schmidt, J.; Gergely, S.; Schönlechner, R.; Grausgruber, H.; Tömösközi, S.; Salgó, A.; Berghofer, E. Comparison of different types of NIR instruments in ability to measure β-glucan content in naked barley. *Cereal Chem.* **2009**, *86*, 398−404.

(10) Pande, R.; Mishra, H. N. Fourier transform near-infrared spectroscopy for rapid and simple determination of phytic acid content in green gram seeds (*Vigna radiata*). *Food Chem.* **2014**, *172*, 880−884.

(11) Parrish, F. W.; Madacsi, J. P.; Phillippy, B. Q.; Wilfred, A. G.; Buco, S. M. Determination of phytic acid in cottonseed by near-infrared reflectance spectroscopy. *J. Agric. Food Chem.* **1990**, *38*, 407−409.

(12) Fulcher, R. G.; O'Brien, T. P.; Lee, J. W. Studies on the aleurone layer 1. Conventional and fluorescence microscopy of the cell wall with emphasis on phenol-carbohydrate complexes in wheat. *Aust. J. Biol. Sci.* **1972**, *25*, 23−34.

(13) Jensen, S.Å.; Munck, L.; Martens, H. The botanical constituents of wheat and wheat milling fractions. I. Quantification by autofluorescence. *Cereal Chem.* **1982**, *59*, 477−484.

(14) Symons, S. J.; Dexter, J. E. Computer analysis of fluorescence for the measurement of flour refinement as determined by flour ash content, flour grade color, and tristimulus color measurements. *Cereal Chem.* **1991**, *68*, 454−460.

(15) Hole, A. S.; Grimmer, S.; Naterstad, K.; Jensen, M. R.; Paur, I.; Johansen, S. G.; Balstad, T. R.; Blomhoff, R.; Sahlstrom, S. Activation and inhibition of nuclear factor Kappa B activity by cereal extracts: role of dietary phenolic acids. *J. Agric. Food Chem.* **2009**, *57*, 9481−9488.

(16) Hole, A. S.; Rud, I.; Grimmer, S.; Sigl, S.; Narvhus, J.; Sahlstrom, S. Improved bioavailability of dietary phenolic acids in whole grain barley and oat groat following fermentation with probiotic *Lactobacillus acidophilus*, *Lactobacillus johnsonii*, and *Lactobacillus reuteri*. *J. Agric. Food Chem.* **2012**, *60*, 6369−6375.

(17) Barnes, R. J.; Dhanoa, M. S.; Lister, S. J. Standard normal variate transformation and de-trending of near-infrared diffuse reflectance spectra. *Appl. Spectrosc.* **1989**, *43*, 772−777.

(18) Martens, H.; Naes, T. *Multivariate Calibration*; Wiley: Chichester, UK, 1989.

(19) Tauler, R. Multivariate curve resolution applied to second order data. *Chemom. Intell. Lab. Syst.* **1995**, *30*, 133−146.

(20) Tauler, R.; Smilde, A.; Kowalski, B. Selectivity, local rank, 3-way data analysis and ambiguity in multivariate curve resolution. *J. Chemom.* **1995**, *9*, 31−58.

(21) Ndolo, V. U.; Beta, T.; Fulcher, R. G. Ferulic acid fluorescence intensity profiles and concentration measured by HPLC in pigmented and non-pigmented cereals. *Food Res. Int.* **2013**, *52*, 109−118.

(22) Kays, S. E.; Shimizu, N.; Barton, F. E.; Ohtsubo, K. Near-infrared transmission and reflectance spectroscopy for the determination of dietary fiber in barley cultivars. *Crop Sci.* **2005**, *45*, 2307−2311.

(23) Lichtenthaler, H. K.; Schweiger, J. Cell wall bound ferulic acid, the major substance of the blue-green fluorescence emission of plants. *J. Plant Physiol.* **1998**, *152*, 272−282.

DOI: 10.1021/acs.jafc.6b04954
J. Agric. Food Chem. XXXX, XXX, XXX−XXX